Supplementary Information for

A Photoswitch Based on Self-Assembled Single Microwire of a Phenyleneethynylene Macrocycle

Jia Luo, Qifan Yan, Yan Zhou, Tian Li, Ningbo Zhu, Chuanjiang Bai, Yong Cao, Jian Wang*, Jian Pei*, and Dahui Zhao*

Beijing National Laboratory for Molecular Sciences, Department of Applied Chemistry, Key Laboratories of Polymer Chemistry and Physics and of Bioorganic Chemistry and Molecular Engineering of the Ministry of Education, College of Chemistry, Peking University, Beijing 10087, Institute of Polymer Optoelectronic Materials and Devices, South China University of Technology, and Key Lab of Specially Functional Materials, Ministry of Education, Guangzhou 510640, China

Email: dhzhao@pku.edu.cn; jianpei@pku.edu.cn

Table of Contents

1. Experimental section

General Procedure's ^{1}H and ^{13}C NMR spectra were recorded on a Varian Mercury plus 300 MHz or a Varian 200 MHz using $CDCl_3$ as solvent unless otherwise stated. All chemical shifts were reported in parts per million (ppm). ^{1}H NMR chemical shifts were referenced to TMS (0 ppm), and ^{13}C NMR chemical shifts were referenced to $CDCl_3$ (77.00 ppm). Absorption spectra were recorded on a PerkinElmer Lambda 35 UV-vis Spectrometer. Photoluminescent (PL) spectra were carried out on a PerkinElmer LS55 Luminescence Spectrometer. MALDI-TOF mass spectra were recorded on a Bruker BIFLEX III time-of-flight (TOF) mass spectrometer (Bruker Daltonics, Billerica, MA, USA) using a 337 nm nitrogen laser with dithranol as matrix. Elemental analyses were performed using a German Vario EL III elemental analyzer. Cyclic voltammetry was performed using BASI Epsilon workstation and measurements were carried out in acetonitrile containing 0.1 M *n*-Bu_4NPF_6 as a supporting electrolyte. Carbon electrode was used as a working electrode and a platinum wire as a counter electrode; all potentials were recorded versus Ag/AgCl as the reference electrode. The scan rate was 50 $mV \cdot s^{-1}$. Optical microscopy was conducted with a Nikon PL-2 microscope. Scanning electron microscopy (SEM) images were obtained with a field emission scanning electron microscope (FESEM, LEO 1530 VP) operated at an accelerating voltage of 1.0 kV. Single crystal was analyzed by a Single Crystal Diffractometer (SMART APEX II, Bruker).

Photoconductor Fabrication and Test:

The glass substrates were cleaned by sonication in acetone for 10 min, followed by 5 min ozone plasma. A thin layer of polystyrene was then spin-coated on the substrate. A solution of macrocycle **1** (1 mg) in hot dioxane (1 mL) was cooled to 0 ^{o}C until the solution was frozen. Then the system was allowed to warm to r.t. and a suspension of microwires of **1** was obtained. This suspension was then dispersed into a large amount of methanol, which was then by spin-coated onto the substrates. The coated substrates were treated at 70 ^{o}C for 8 hours under vacuum. A polyethylene (PE) fiber with a diameter of 20 μm was mounted on the substrate as a shadow mask, and a

layer of 150 nm gold was deposited onto the substrate by thermal evaporation under the pressure of 4×10^{-4} Pa at 0.3–1.0 Å•s^{-1} before the fiber mask was removed. The photoconductor based on a single microwire was tested in ambient atmosphere using an Agilent 4155C semiconductor parameter analyzer connected to a Cascade RF1 manual probe station. The irradiation light was provided by a Newport CL-2000 diode pumped crystal laser with a wavelength of 405 nm. The laser beam was directed through a small fixed iris and reflected onto the microwire by a set of mirrors, with a final beam diameter of ~0.6 mm. To measure the light intensity *in situ*, a small fraction of the beam was split by a beam splitter and reflected onto an 818-ST-UV photodiode connected with an 841-PE power meter. The beam intensity was obtained by dividing the beam power by the spot size.

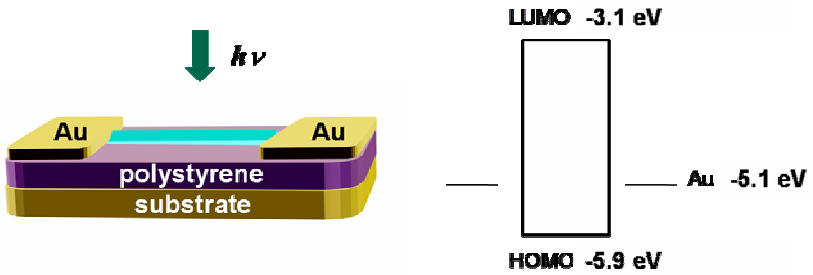

Figure S1. Schematic representation of a photoconductor device (left) and HOMO LUMO energy levels of macrocycle **1** relative to the Au Fermi level.

*Synthesis and Characterization of Macrocycle **1**:*

Macrocycle **1** was prepared following a synthetic route as shown below (Scheme S1). The procedures used were similar to those of a previously reported macrocycle of the same backbone structure but with longer (dodecyloxy) side chains.[1]

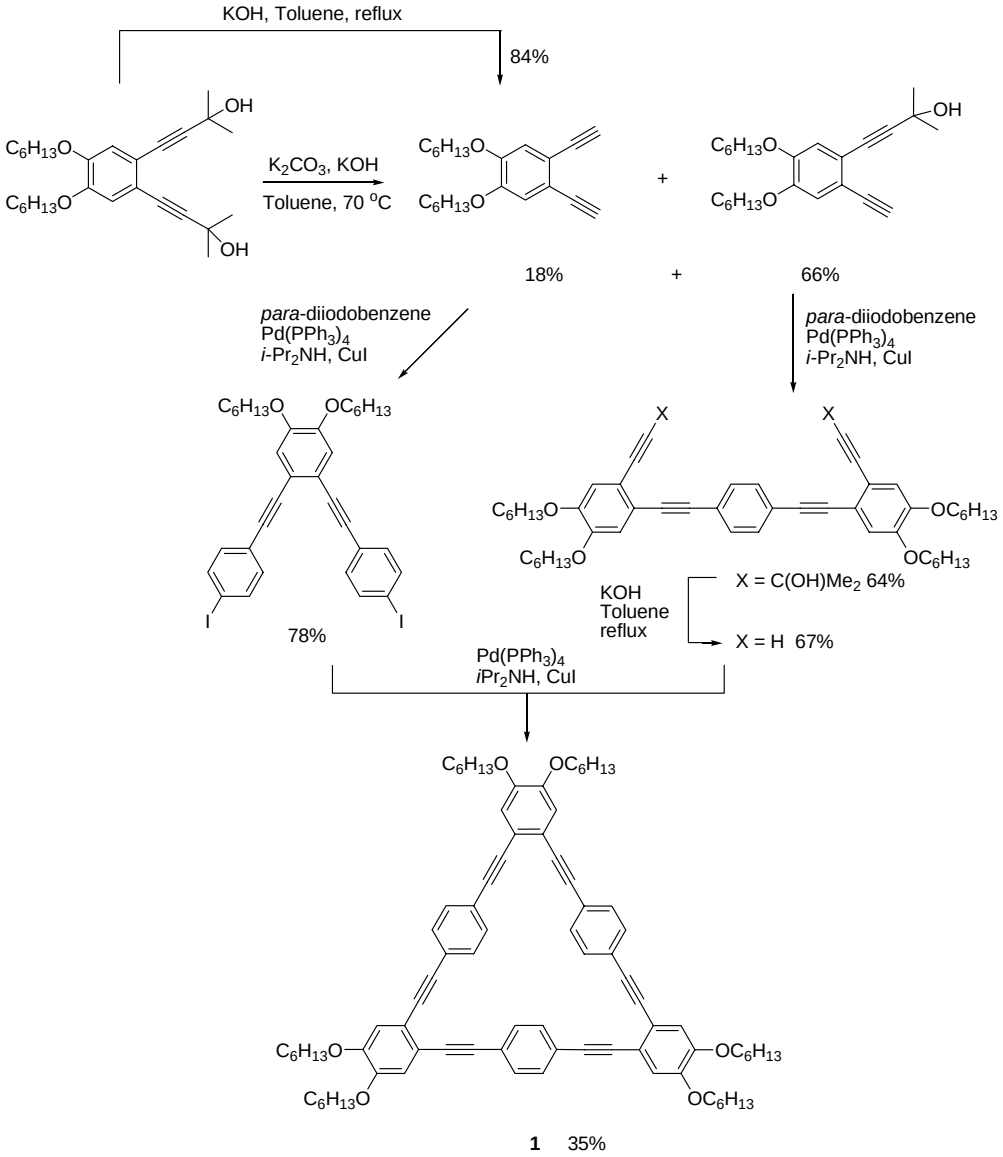

Scheme S1. Synthesis route for macrocycle **1**

Characterization data of macrocycle **1**: ^{1}H NMR (300 MHz, $CDCl_3$, ppm): δ 7.56 (s, 12H), 7.04 (s, 6H), 4.04 (t, 12H, J = 6.6 Hz), 1.83-1.88 (m, 12H), 1.47-1.50 (m, 12H), 1.33-1.40 (m, 24H), 0.90-0.95 (m, 18H). ^{13}C NMR (50 MHz, $CDCl_3$, ppm): δ 149.6, 131.6, 123.5, 118.8, 115.9, 92.2, 90.9, 69.4, 31.7, 29.2, 25.8, 22.8, 14.2. MS (MALDI-TOF): Calcd. for $C_{84}H_{96}O_6$: 1200.7; Found: 1200.6 (M^+). Anal. Calcd. for $C_{84}H_{96}O_6$: C, 83.96; H, 8.05. Found: C, 83.58; H, 7.92 (sample was re-crystallized from a $CHCl_3$/CH_3OH co-solvent).

2. Optical microscope and SEM images of the microwires

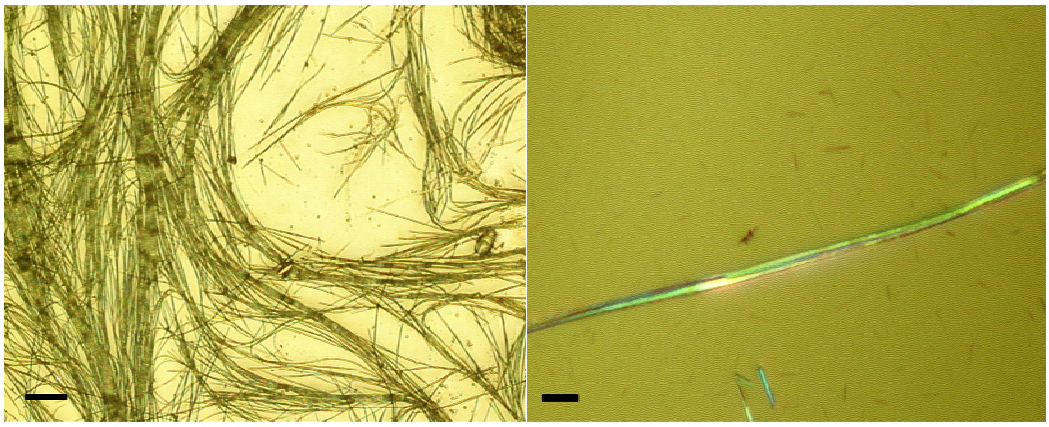

Figure S2. Optical microscopy images of microwires of **1**; the image on the right was taken under cross-polarized light; the scale bar stands for 20 μm (left) and 5 μm (right), respectively.

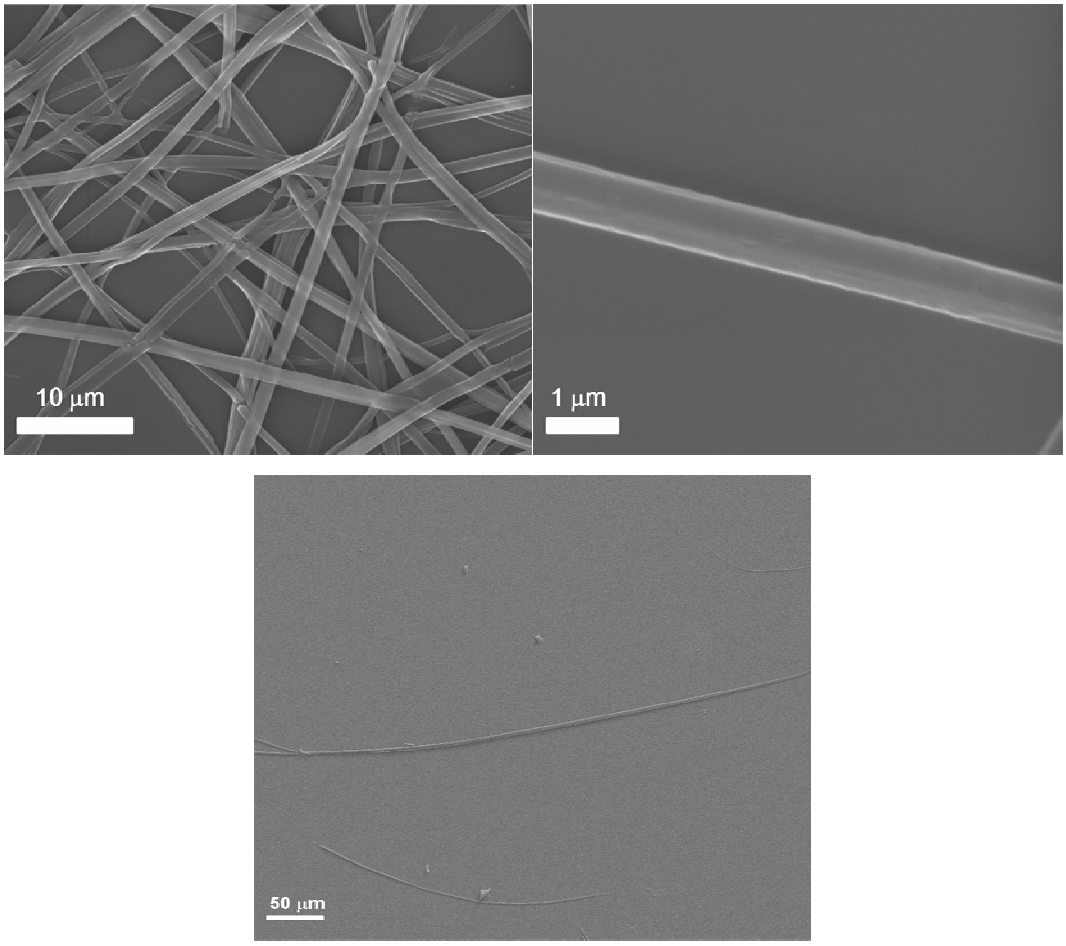

Figure S3. Scanning electron microscopy (SEM) images of microwires deposited on silica substrates.

3. Photophysical characterization of macrocycle 1

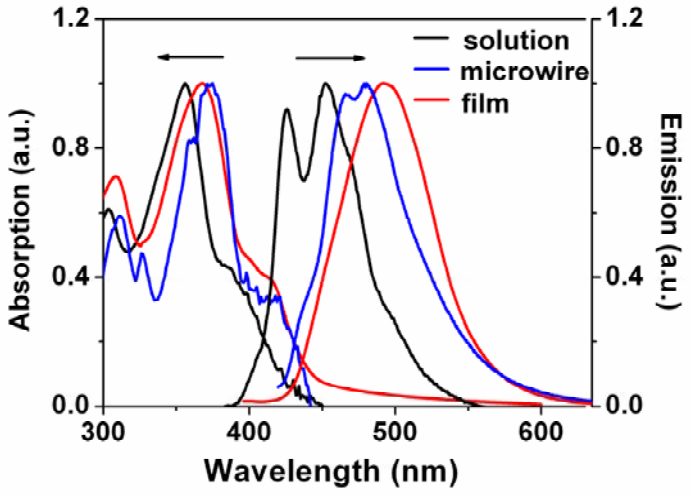

Figure S4. UV-vis absorption and emission spectra of macrocycle **1** in dilute solution of THF, as pristine films cast from dilute THF solution, and as microwires self-assembled from dioxane solution.

4. Crystal structure analyzed by single crystal XRD

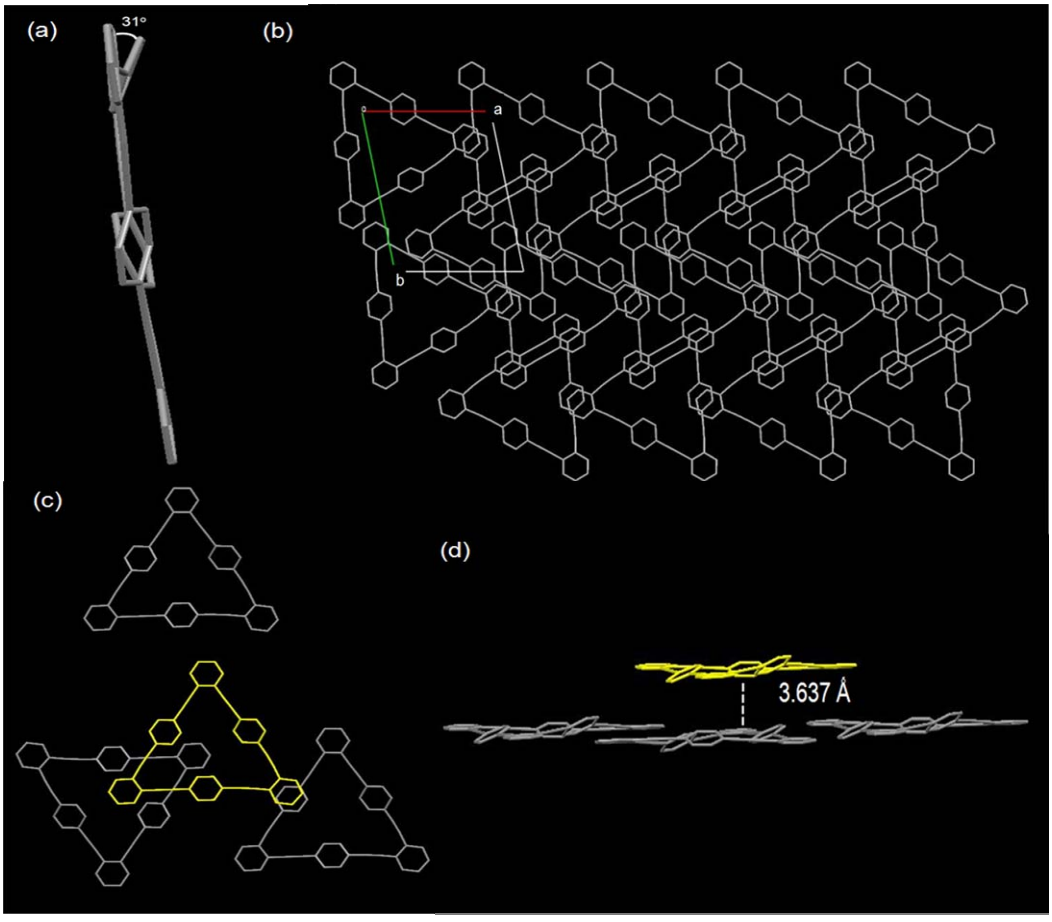

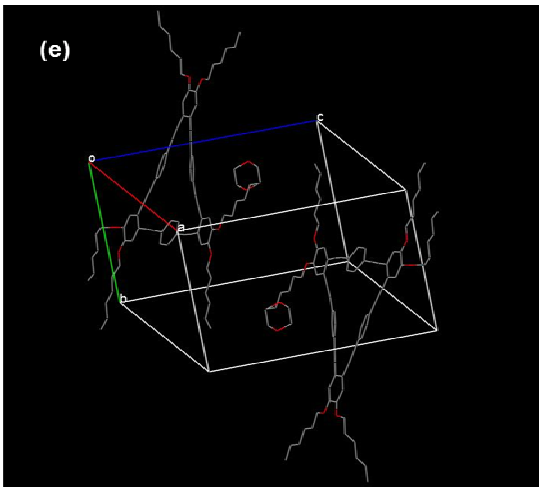

Figure S5. Crystal structure of **1**: (a) a torsional angle of ca. 31º between the *p*-phenylene ring and the macrocycle plane; (b) view along the crystallographic *c*-axis; (c) top view and (d) side view along the macrocycle plane, the side chains, hydrogen atoms and solvent molecules have been omitted for clarity; (e) packing of macrocycles in a unit cell with two dioxane molecules contained.

Macrocycle **1** forms a triclinic lattice, with a space group *P-1* and the unit cell dimensions of a = 13.4266(6) Å, b = 14.7760(7) Å, c = 20.1053(9) Å, α = 84.8020(10)°, β = 71.9290(10)°, and γ = 76.2150(10)°. The planes of macrocycles partly overlapped with one another, rather than forming columnar structures by stacking in a "face-to-face" fashion.[2]

5. Photoconductive behaviors of single microwires

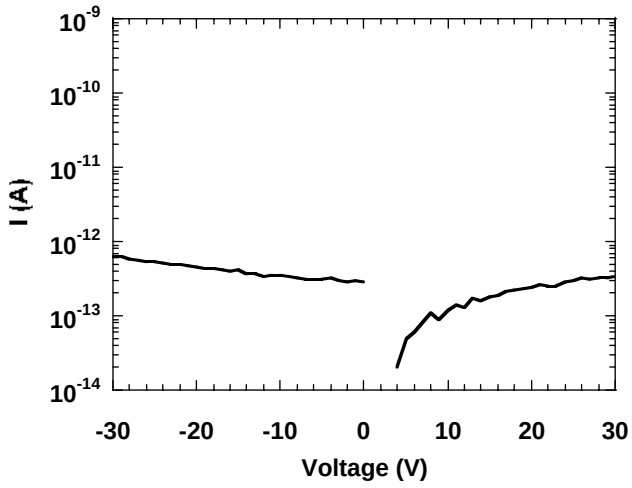

Figure S6. *I-V* curve of a typical device of a single microwire under dark conditions.

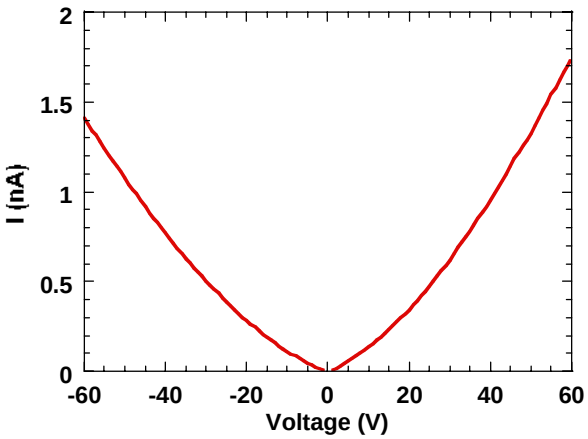

Figure S7. *I-V* curve of a typical device of a microwire under illumination (intensity = 85 mW/cm^2).

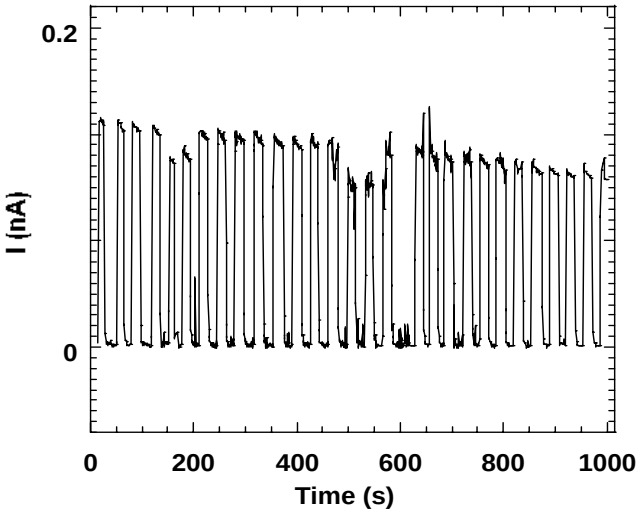

Figure S8. On/off cycles of a typical photoconductor device of a microwire with 30 V bias and light intensity of 85 mW/cm^2.

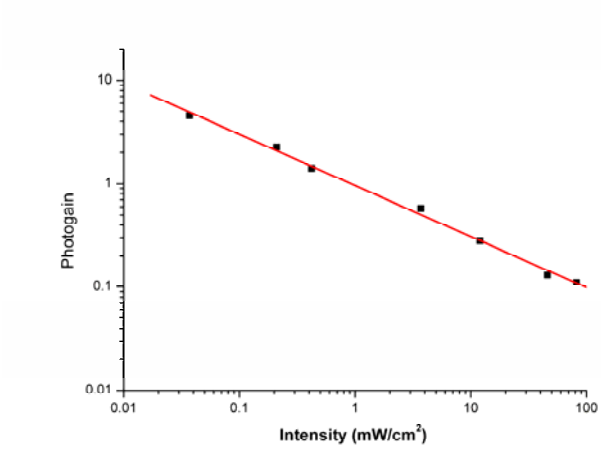

Figure S9. Photogain dependence on the light intensity in devices of microwires at a bias of 30 V.

6. Differential scanning calorimetric trace of macrocycle 1

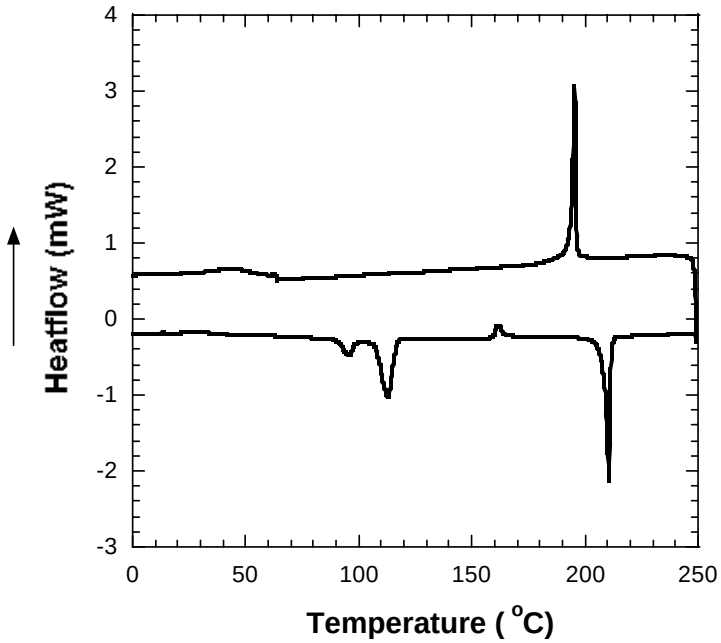

Figure S10. DSC trace of macrocycle **1**

7. Temperature dependent emission spectra of microwires

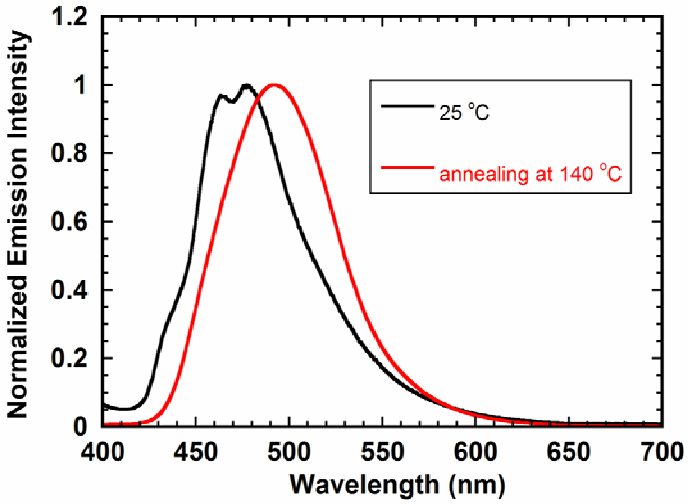

Figure S11. Emission spectra of microwires at different temperatures

8. Comparison of photoconductivity between microwires and single crystal rods

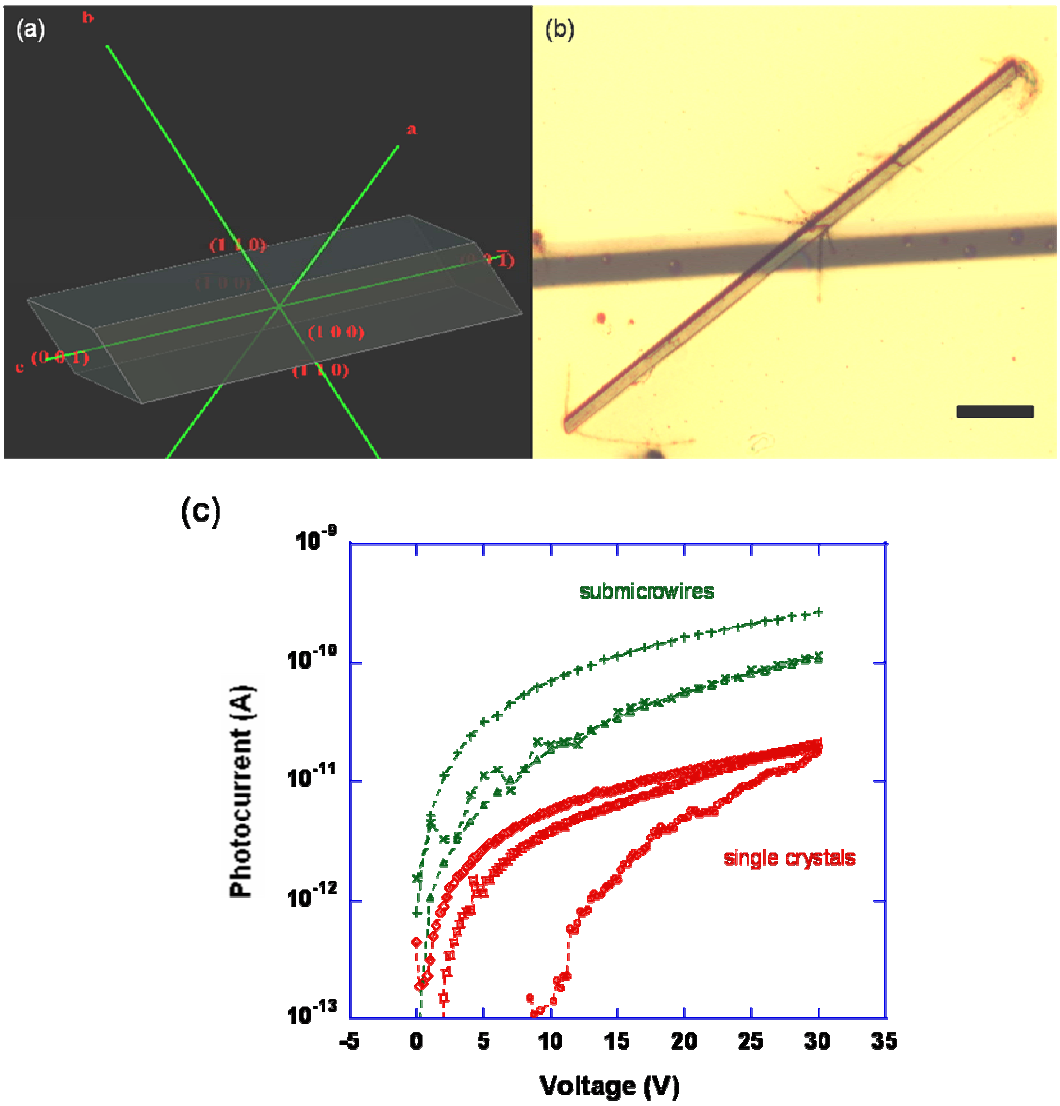

Figure S12. (a) The orientation of a single crystal simulated using WinXMorph software[3] via the Bravais-Friedel-Donnay-Harker (BFDH) method.; (b) a device based on a single crystal rod (the scale bar stands for 40 μm); (c) *I-V* curves of representative devices based on single crystal rods (red lines) and microwires (green lines) under the same illumination density (85 mW/cm^2).

The BFDH model identifies the crystal faces and long crystallographic axis of the crystal. Model was drawn with the WinXMorph software (Kaminsky, 2004). From the simulation, the π-π stacking takes place along the long axis of the crystal (although a small tilt angle exists between stacking direction and the *c*-axis). According to the photoconductivity behaviors of two types of structures, the photocurrent density of the

microwires was apparently higher than that of single crystal rods considering the smaller cross-section of microwires. Therefore, the carrier generation and transport processes are more efficient in the microwires than in single crystal rods.

9. *I-V* curves of microwire photoconductor after annealing at 140 °C

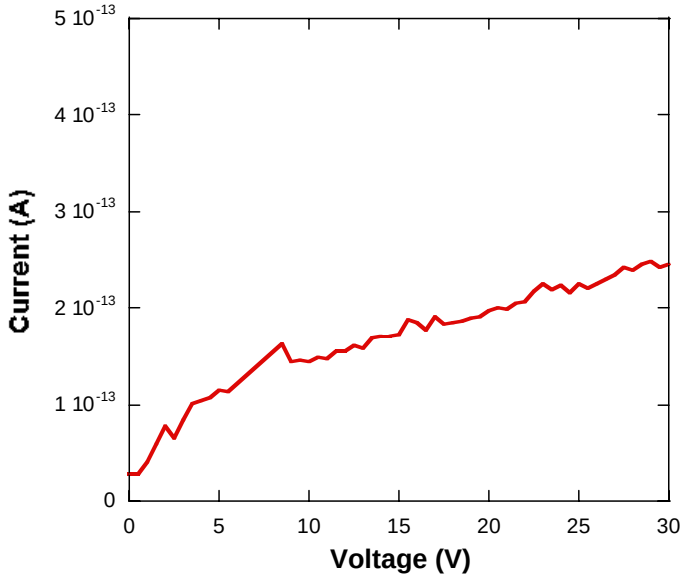

Figure S13. *I-V* curves of microwire photoconductor at columnar phase.

References:

1. Zhu, N.; Hu, W.; Han, S.; Wang, Q.; Zhao, D. *Org. Lett.* **2008**, *10*, 4283.
2. Hisaki, I.; Sakamoto, Y.; Shigemitsu, H.; Tohnai, N.; Miyata, M.; Seki, S.; Saeki, A.; Tagawa, S. *Chem. Eur. J.* **2008**, *14*, 4178.
3. Kaminsky, W. *J. Appl. Crystallogr*. **2005**, *38*, 566.

Copy of ^{1}H NMR spectrum of **1**

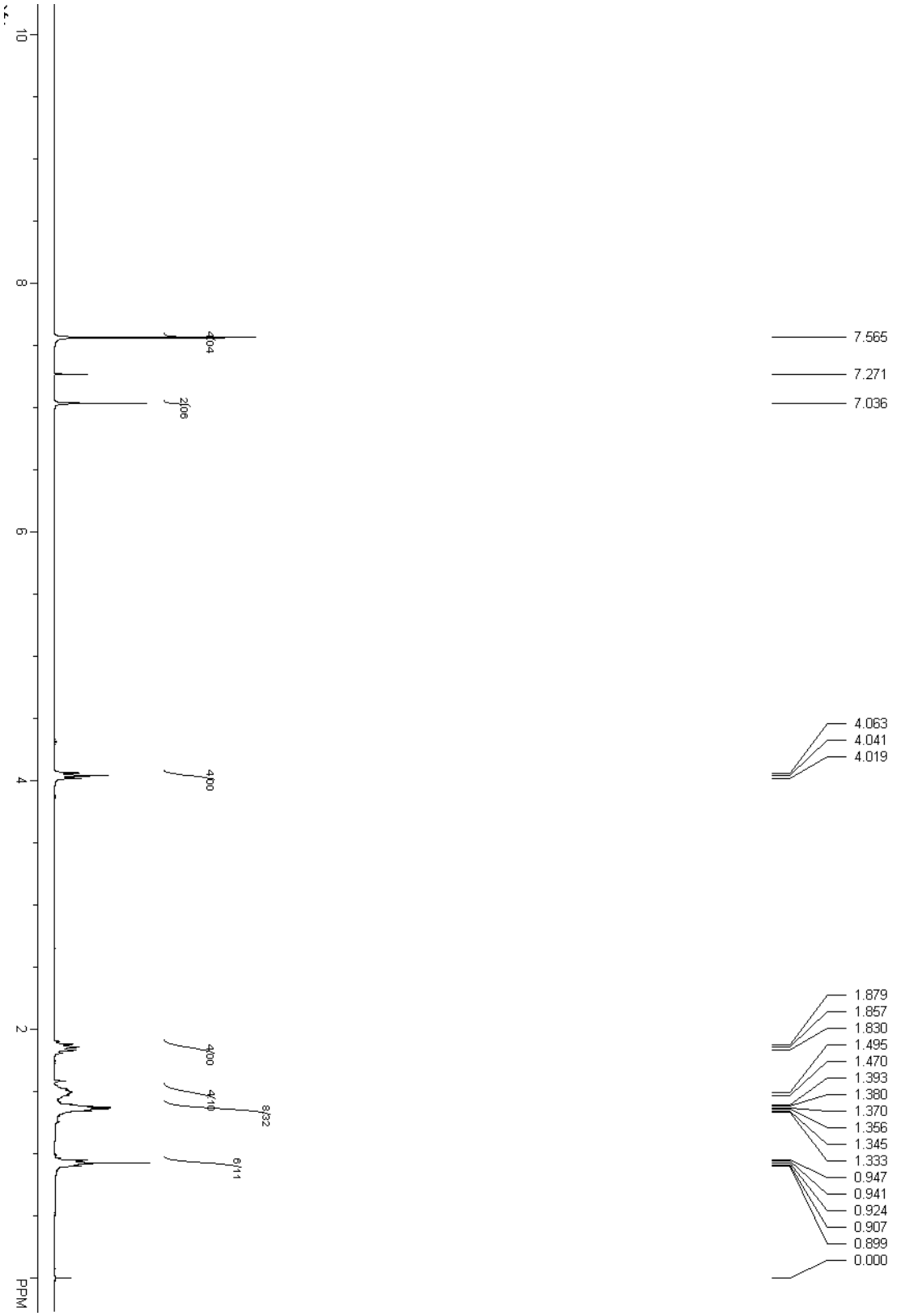

Copy of ^{13}C NMR spectrum of **1**

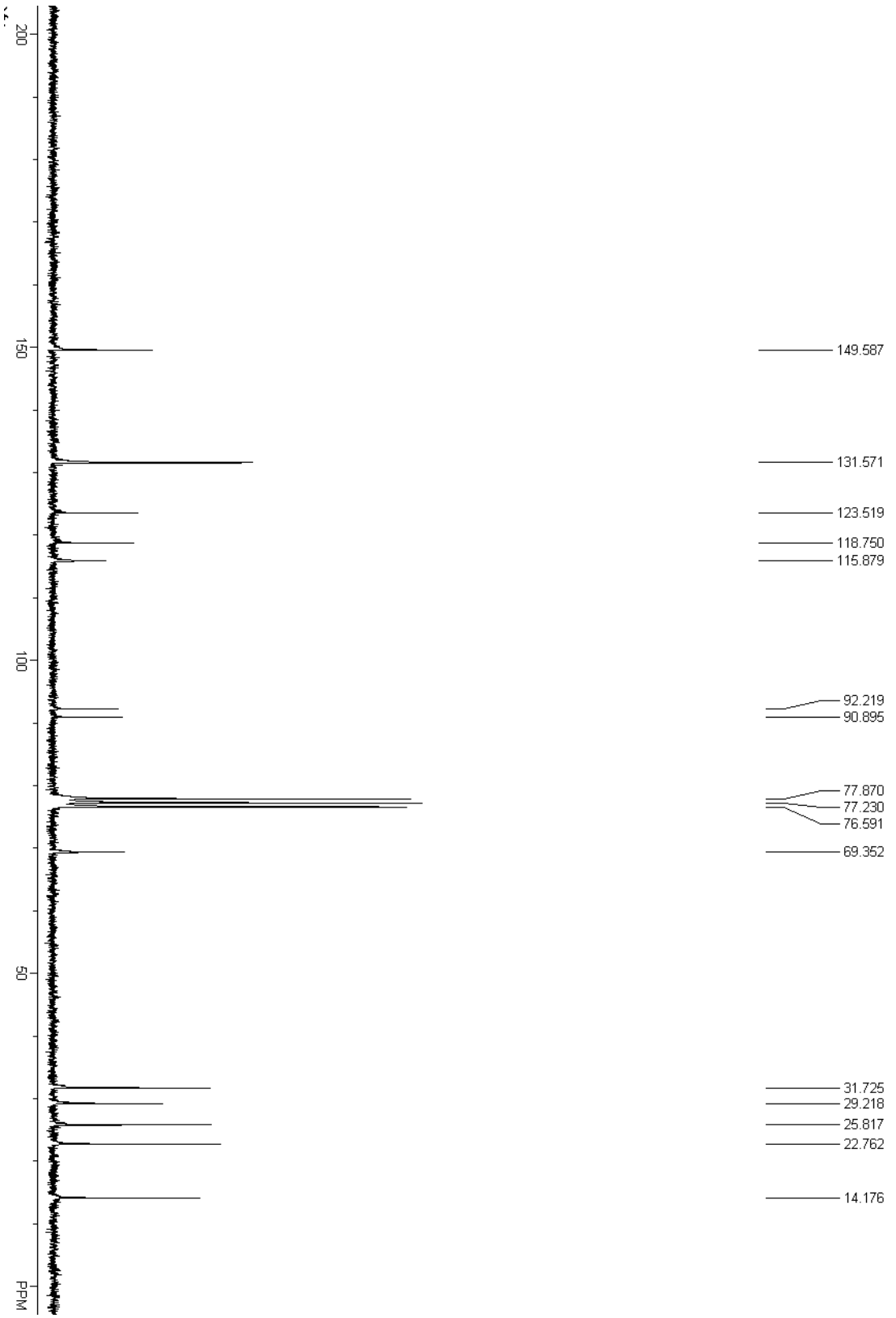

MALDI-TOF MS:

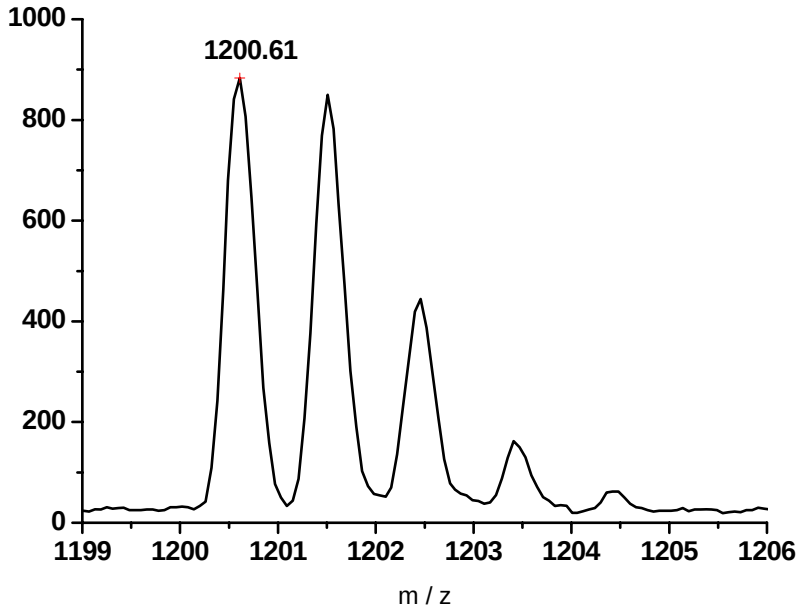
1200.61
1000
800
600
400
200
0
1199
1200
1201
1202
1203
1204
1205
1206
m / z